

Integral Model of COVID-19 Spread and Mitigation in UK: Identification of Transmission Rate

Natali Hritonenko^a, Caroline Satsky^b and Yuri Yatsenko^c

^a*Department of Mathematics, Prairie View A&M University*
Prairie View, 77446 Texas, USA

^b*Department of Mathematics and Statistics, Texas Tech University*
Lubbock, 79401 Texas, USA

^c*Dunham College of Business, Houston Baptist University*
Houston, 77074 Texas, USA

E-mail(*corresp.*): nahritonenko@pvamu.edu

E-mail: caroline.satsky@ttu.edu

E-mail: yyatsenko@hbu.edu

Received October 1, 2021; revised September 18, 2022; accepted September 19, 2022

Abstract. The integral model with finite memory is employed to analyze the timeline of COVID-19 epidemic in the United Kingdom and government actions to mitigate it. The model uses a realistic infection distribution. The time-varying transmission rate is determined from Volterra integral equation of the first kind. The authors construct and justify an efficient regularization algorithm for finding the transmission rate. The model and algorithm are approbated on the UK data with several waves of COVID-19 and demonstrate a remarkable resemblance between real and simulated dynamics. The timing of government preventive measures and their impact on the epidemic dynamics are discussed.

Keywords: integral epidemiologic models, COVID-19 mitigation, Volterra integral equations, ill-posed problems, regularizing algorithm.

AMS Subject Classification: 92D30; 92C60; 45D05; 45G15; 00A71.

1 Introduction

The COVID-19 pandemic triggered a flood of research attempts to simulate the dynamics and control of COVID-19 epidemics in various countries. Most

of them use well-known SIR and SEIR epidemic models to describe the impact of government actions and changing social practices on the epidemic spread. However, specifics of COVID-19 require more accurate models and data processing methods to describe and control it. Indeed, it is well known [4] that the standard SIR and SEIR models do not adequately describe transmission patterns of real diseases, including COVID-19. A variety of advanced epidemiologic models has been developed to address this deficiency [9, 12, 14, 15, 25, 26]. Most of them have not been applied to COVID control yet.

Detailed data about COVID-19 pandemic in different countries are publicly available from many reliable web-based sources. However, the major challenge is that all those data are reported with errors. It necessitates the development of special algorithms for COVID-19 epidemic simulation and control. The present paper develops such algorithms for a new flexible model of epidemic control successfully tested on the COVID-19 dynamics in the US over one-year period [16]. The model is described by Volterra integral equations [3, 11, 17, 18, 19] and contains SIR, SEIR, and some other epidemic models [15] as special cases. It accurately depicts the COVID-19 infectivity pattern from clinical data. The present paper provides a systematic analysis of available data, develops a new identification algorithm for model identification and applies it to the COVID-19 dynamics in the United Kingdom.

Integral equations are more general and natural in mathematical modeling of epidemics as compared to the ODEs [9, 10, 15, 21, 22]. They represent an alternative way to develop realistic descriptions of epidemic propagation and control. The integral equations appeared early in mathematical modeling of populations in the groundbreaking works [30] of Volterra and [22] of Kermack and McKendrick. First attempts to model real populations using ODEs demonstrated that the population growth rates did not respond instantaneously to changes in population sizes. To address this fact, Vito Volterra added integral delay terms to differential models of population dynamics. More details about classic and comprehensive integral models of populations can be found in the monographs [3, 9, 11, 19, 21]. Despite this early interest, the analysis and applications of integral models with delays have lagged behind ODE-based models that do not incorporate delays. On the other hand, the importance of time delays is recognized in mathematical epidemiology [26]. Integral dynamic models with distributed delays [11, 19, 20] have been known for almost a hundred years and successfully used in many applications. Such models are more natural and flexible for the control of COVID-19 [15]. They open new possibilities to describe and optimize the economic control of epidemics.

An imperative goal of COVID-19 research is to assess the effectiveness of the government actions and preventive measures in mitigating the epidemic spread. Related models use changes of the transmission rate to capture public measures to control COVID-19. In the integral model [16], finding the time-varying transmission rate requires solving the Volterra integral equation (VIE) of the first kind. Such equations belong to the ill-posed problems, in which small variations of given data can lead to large changes in unknown variables [23]. There exist many regularization methods suitable for solving this identification problem. However, specialized nature of the COVID-19 epidemic suggests their

particularly effective modifications. Specifically, the latent period of COVID-19 pandemic requires some adjustments though allows more accurate modeling.

The novel theoretic contribution of this paper is the data analysis and effective regularization algorithm for identification of the time-varying transmission rate of COVID-19 epidemics. The used methodology combines direct discretization techniques and a continuous regularization method that preserves the Volterra structure of the original model and takes advantage of its formulation as an integral model with finite lags. The developed algorithm is successfully applied to simulate and analyze the COVID-19 spread and control in the UK in 2020-21, which determines the applied significance of the paper.

The paper is as follows. Section 2 presents the model. Section 3 describes the identification algorithm for time-varying transmission rate. Section 4 applies the model and algorithm to the COVID-19 epidemic in the UK and compares the simulated dynamics and timing of related government actions. Section 5 concludes and provides directions of future research.

2 Integral model for epidemic control: formulation and properties

Let us consider the following integral model of epidemics:

$$I(t) = \int_{t-T}^t b(u, t-u) I(u) \frac{S(u)}{N} f(t-u) du, \quad (2.1)$$

$$S(t) = N - \int_{-T}^t b(u, t-u) I(u) \frac{S(u)}{N} du, \quad (2.2)$$

$$R(t) = N - I(t) - S(t), \quad 0 \leq t < \infty, \quad (2.3)$$

first introduced in [16]. The model describes the dynamics of three groups of individuals: S (susceptible), I (infectious), and R (recovered or dead). Here, N is the constant population size and $T > 9$ is the maximal duration of the infectiousness period. In real life, the time T is finite.

The key model function $b(u, s) \geq 0$, $0 < u < T$, describes the infectiousness intensity (transmission rate) that depends on the contact time u and the time s passed after the infection occurs, $b(u, s) = 0$ for $s > T$. The dependence of the infection intensity b on the time-since-infection s is a major concern in modern epidemic models [3, 9]. The model (2.1)–(2.3) is flexible and can describe any realistic distribution of infectious periods [25].

The given $f(s) \geq 0$ is the fraction of population that still remain infectious at time s , $f(0) = 1$, $f(s) = 0$ for $s > T$. All recovered individuals are assumed to become immune, so, the only susceptible fraction S/N of the population can become infected. The fraction $0 < \delta < 1$ of "recovered or dead" dies, so, the total number of deaths is

$$D(t) = \delta R(t).$$

As proven in [16], assuming continuous functions b and f , the nonlinear Volterra integral equations of the second kind (2.1)–(2.3) have a unique non-negative

solution $I(t)$, $S(t)$, $R(t)$, $0 < T < \infty$, at the given initial conditions

$$I(t) = \tilde{I}_0(t), \quad S(t) = \tilde{S}_0(t), \quad t \in (-T, 0]. \quad (2.4)$$

The most important feature of the integral model (2.1)–(2.3) is that it can describe any pattern $b(u, s)$ of infectivity and latency, which is not possible in ODE-based models.

2.1 Infectiousness distribution, transmission rate, and survivor distribution

Following [16], we assume that the infectiousness intensity $b(u, s)$ is the product of two functions

$$b(u, s) = \beta(u)\tilde{\beta}(s), \quad 0 \leq t < \infty, \quad 0 \leq s \leq T, \quad (2.5)$$

to emphasize fundamental differences in its dependence on the infection time u and time-since-infection s . Then, the Equation (2.1) becomes

$$I(t) = \int_{t-T}^t \beta(u)I(u) \frac{S(u)}{N} \tilde{\beta}(t-u)f(t-u)du, \quad 0 \leq t < \infty. \quad (2.6)$$

Solving the integral Equation (2.6) with respect to the unknown $\beta(s)$ under noisy data is the major subject of this paper.

The infectiousness distribution $\tilde{\beta}(s)$ of infection intensity over the period $[0, T]$ is critical in mathematical epidemiology. All contemporary epidemic models have been designed to describe more accurate infectiousness period distributions of real epidemics. In theory, $\tilde{\beta}(s)$ may be of any distribution, from exponential to uniform distribution [25]. In practice, it is determined from detailed clinical data over a certain period $[0, T]$ (see Section 3).

The dependence of $b(u, s)$ on the infection time u determines the *time-dependent transmission rate* $\beta(u)$, that attracts an increasing interest during COVID-19 time. Starting 2020, numerous epidemic-economic models attempt to simulate of COVID-19 epidemic and government attempts to mitigate it. Thus, [1, 2, 5, 13], and others use the time-dependent transmission rate $\beta(t)$ in SIR and SEIR models to capture how government decisions to lockdown and re-open the economy affect the epidemic spread.

However, it is well known in contemporary epidemiologic research that the standard SIR and SEIR models do not adequately describe real transmission delays for many diseases [25]. In particular, the infectiousness distributions $\tilde{\beta}(s)$ in those models have too fat right tail and are unrealistic. Following such exponential distributions, some individuals will remain infectious at any distant future time. Importance of COVID-19 pandemic requires more advanced models to describe and control it.

The integral model (2.1)–(2.3) with finite memory accurately portrays delays in the variable transmission rate $\beta(t)$ to capture government control of COVID-19. It depicts real patterns of infectivity and latency, obtained in clinical data.

The survivor distribution $f(s)$, $s \in [0, T]$, in (2.1)–(2.3) describes the fraction of individuals that remain infectious s days after becoming infected. In practice, it decreases from $f(0) = 1$ at the beginning to $f(T) = 0$ at the end of the finite infectiousness period $[0, T]$. It should be also based on detailed clinical data, if available. As demonstrated in [16], the shape of f affects simulation outcomes less seriously compared to the infectiousness period distribution $\tilde{\beta}$.

2.2 Reproduction number

The most publicly known epidemiological parameter is the *reproduction number* R_t that defines the expected number of new infections generated by one infected individual. Its distinguished feature is that the number I of infected increases when $R_t > 1$ and decreases when $R_t < 1$ [14, 21]. The UK government regularly refers to the reproduction number to describe COVID-related goals and actions of UK government to control epidemic [7].

The number R_t is related to the transmission coefficient β and is calculated differently in different epidemic models. Following [16], the reproduction number in the integral model (2.1)–(2.3) is

$$R_t = \int_{t-T}^t b(u, t-u) \frac{S(u)}{N} f(t-u) du. \tag{2.7}$$

The basic reproduction number

$$R_0 = \int_{t-T}^t b(u, t-u) f(t-u) du$$

describes the expected number of new infections generated by one infected in a totally susceptible large population at the beginning of epidemic, i.e., when $I(t) \ll N$ and $S(t) \sim N$.

3 Identification of integral model on COVID-19 data

This section determines the unknown time-dependent transmission rate $\beta(t)$ from the integral model (2.1)–(2.3), (2.6), assuming that the variables $S(t)$, $I(t)$, and $R(t)$ are known over a long enough interval $[T_0, T_{\max}]$.

3.1 Data set description

Following recent clinical research [29], the infectiousness period distribution $\tilde{\beta}(s)$ for COVID-19 is described by the solid black curve in Figure 1 taken from [16]. This shape of $\tilde{\beta}(s)$ is common for influenza-like diseases, see Figure 13.1 in [26]. For comparison, Figure 1 also shows the theoretic infectiousness distributions (2.5)–(2.7) for the SIR, SEIR, and the multi-compartment Erlang SIR model at $n = 2$ and $n = 5$. As seen in Figure 1, $\tilde{\beta}(s)$ is very small at $s > 14$ days. So, we choose the COVID-19 infectiousness interval of $T = 14$ days, that includes both latent (four days) and infectious periods of the COVID-19 infected individuals.

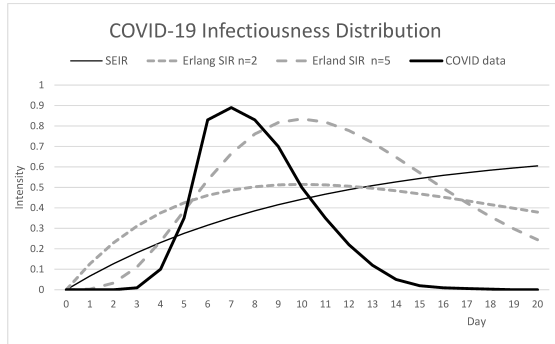


Figure 1. Dependence of infectivity on the *time-since-infection* for COVID-19 clinical data (bold black line), SEIR distribution, and Erlang distribution [19].

The COVID-19 data for the UK over the time horizon of April 2020 – May 2021 is taken from the reliable web-based source [27]. The given function $I(t)$ corresponds to the column “Daily new confirmed COVID-19 cases per million people” and is shown in Figure 2.

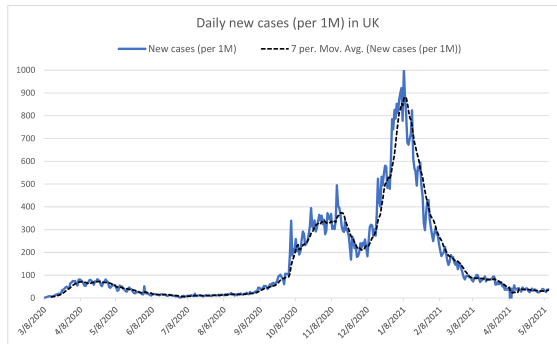


Figure 2. The dynamics of new infected individuals in the UK for April 2020 – May 2021, taken from (Our World in Data 2020).

So, $N = 10^6$ in (2.1)–(2.3). One can see that it has frequent sharp fluctuations apparently caused by data reporting errors. This is a well-known common problem for COVID-19 data [8]. For this reason, we use “Daily new confirmed COVID-19 cases per million people (the rolling 7-day average)” in our simulation. Preliminary smoothing and filtering data is a common approach before using discretization methods, especially for ill-posed problems [24].

Several special cases of the survivor distribution f with a finite $T > 0$ are provided in [16]. We choose the uniform survivor distribution

$$f(s) = \begin{cases} 1, & 0 \leq s < T, \\ 0, & s \geq T \end{cases}$$

in accordance with which infected individuals remain infectious exactly T days after becoming infected and then they immediately move to the stage R . Then, two-week delayed “Total confirmed COVID-19 cases (per 1 M)” minus “Daily confirmed COVID-19 deaths (per 1 M)” can be used as a proxy for $R(t)$. Our numeric experiments show that the survivor distribution $f(s)$ appears to be less essential than $\tilde{\beta}(s)$. Choosing a different $f(s)$ leads to similar simulation results.

3.2 Challenges in solving identification problem

Because of the COVID-19 latent period, the given $\tilde{\beta}(s) = 0$ at $0 \leq s \leq \tau$, where $\tau = 3$ days (see Figure 1). To highlight this fact, we rewrite the Volterra integral equation of the first kind (VIE-I) (2.6) for the unknown $\beta(t)$ as

$$I(t) = \int_{t-T}^{t-\tau} \beta(u)I(u)\tilde{\beta}(t-u)\frac{S(u)}{N}f(t-u)du, \quad t_0 \leq t \leq T_{max}. \tag{3.1}$$

If we have known exact functions I , f , and $\tilde{\beta}$ in the Equation (3.1), then its numeric solution would have been trivial. The challenge is that all COVID-19 data are reported and known with errors [23]. Such errors are clearly visible in the graph of I in Figure 2 even after the seven-day smoothing. This is the only real data available.

The linear VIE (3.1) belongs to the category of ill-posed (ill-conditioned) problems, in which small variations of given data can lead to large changes in unknown variables. It can be solved using various regularization algorithms, see [6, 23] and the references therein. The regularization theory for linear ill-posed problems is well-developed. To better discuss the nature of regularization, let us convert (3.1) to a more standard VIE-I form. Introducing the new unknown variable x and given convolution kernel K as

$$x(t) = I(t)S(t)\beta(t)/N, \quad K(u) = \tilde{\beta}(u + \tau)f(u + \tau), \tag{3.2}$$

and replacing the independent variable $t \rightarrow t + \tau$, the Equation (3.1) becomes a convolution VIE-I with finite distributed delay

$$\int_{t-\hat{T}}^t K(t-u)x(u)du = I(t + \tau), \quad t_0 - \tau \leq t \leq T_{max} - \tau, \tag{3.3}$$

with respect to x , where $\hat{T} = T - \tau > 0$ is the delay duration [19, 20]. To find a unique solution $x(t)$ of the delay Equation (3.3) for $t_0 - \tau + \hat{T} < t \leq T_{max} - \tau$, we need to know or approximate the initial function

$$x(t) = x_0(t), \quad t \in [t_0 - \tau, t_0 - \tau + \hat{T}]$$

on the process prehistory.

Solving the ill-posed Equation (3.3) has serious challenges in the situation when we know only an approximation I^δ of the given function I . This is exactly what happens with COVID-19 data. As in [23], we assume here and thereafter that $K \in C[0, T]$ and the given function I is such that there exists a unique

solution $x \in U = L_2(0, T)$ of the integral equation (3.3). Let $I^\delta \in U$ satisfy $\|I - I^\delta\|_U < \delta$ for some $\delta > 0$. Formally, the ill-posedness of the Equation (3.3) means that its solution x^δ with a perturbed I^δ (if such a solution exists) may be arbitrarily far from the solution x of the unperturbed problem (3.3).

The aim of regularization algorithms is to find an approximate solution of the Equation (3.3) that is stable under small changes in given functions. Namely, the regularization algorithm defines a *regularized* approximate solution x^δ of the Equation (3.3) in such a way that the solution x^δ approaches the desired exact solution x (in the metric of U), when the initial data error $\delta \rightarrow 0$. The regularization algorithm usually includes finding appropriate regularization parameters from supplementary information about the problem, such as the accuracy of initial data.

Following [23], we focus on the regularization methods of Volterra type that retain the causal nature of Volterra operator in (3.3). Specifically, we choose a simple and effective regularization technique, the singular perturbation approach, first offered in [28]. This technique adds the regularizing term $\alpha\beta(t)$, $\alpha > 0$, to the LHS of the Equation (3.3), which makes it the VIE-II:

$$\alpha x(t) + \int_{t-\hat{T}}^t K(t-u)x(u)du = I(t+\tau), \quad t_0 - \tau \leq t \leq T(\max) - \tau. \quad (3.4)$$

The role of the regularizing term and the choice of the regularizing parameter α are discussed below, but here we shall note that adding it directly to the original delayed equation (3.1) would make the regularization much less effective.

3.3 The degree of Ill-posedness of VIE-I

A classic technique to solve VIEs of the first kind is to differentiate them, which frequently leads to well-posed VIEs of the second kind [11]. However, the Equation (3.3) after differentiation becomes

$$K(0)x(t) - K(T)x(t-T) + \int_{t-T}^t K'(t-u)x(u)du = I'(t+\tau) \quad (3.5)$$

and remains the VIE-I because $K(0) = f(\tau)\tilde{\beta}(\tau) = 0$ by (3.2). The equation of the first kind (3.3) is worse for numeric solution than (3.5) because it contains the derivatives of K and I . To discuss the "degree of ill-posedness" of various first-kind equations, Lamm [23] introduced the concept of a v -smoothing problem. Applied to the VIE-I (3.3), this concept is described by the following definition.

DEFINITION 1. The Volterra equation (3.3) is a v -smoothing problem with an integer $v \geq 1$ if $I \in C^v[t_0, t_{\max}]$, $K \in C^v[0, T]$, $K^{(l)}(0) = 0$ at $l = 0, \dots, v-2$, and $K^{(v-1)}(0) \neq 0$ for $t \in [0, T]$.

Following this definition, the Equation (3.3) on our COVID-19 dataset is a v -smoothing problem with $v \geq 2$ since $K(0) = 0$. As noted in [23], the vast amount of theoretical analysis for regularization methods is restricted to one-smoothing Volterra problems, which are the least ill-posed.

Common results of the regularization theory are the convergence theorems that provide conditions on the selection of the regularization parameter $\alpha = \alpha(\delta)$ so that $x^\delta \rightarrow x$ in U as $\delta \rightarrow 0$. The convergence theorem for the single perturbation regularization of the standard VIE-I is well known at $v = 1$ but is still an open issue if $v > 1$ [23]. We do not pursue the convergence theory for the (3.3) \rightarrow (3.4) regularization for two reasons:

- The convergence theorems state how to select $\alpha = \alpha(\delta)$ asymptotically as $\delta \rightarrow 0$, but do not provide a rule for selecting α when only one particular perturbation I^δ of I is known.
- Because the COVID-19 data is discrete, we must combine a continuous regularization method of Volterra-type with an effective discretization technique using a proper numeric integration rule.

Instead, we develop a numeric algorithm based on the direct discretization of the regularized Equation (3.4) and approximate it on the real COVID data.

3.4 Regularizing algorithm

Our regularizing algorithm for the Equation (3.4) includes iterations through two linked stages:

- Discretization of the regularized equation (3.4) at a chosen value α .
- Verification of the obtained solution using correspondence to original data.

At the end of Stage 2, we select a new corrected value α of regularizing parameter and repeat Stage 1 if needed. Several successive iterations allow reaching the best possible visual correspondence between calculated and original data.

Stage 1. Discretization of the regularized integral equation (3.4).

In the COVID-19 dataset described in Section 3.1, the discrete functions (vectors) $S(t)$, $I(t)$, and $R(t)$ are known over the interval $[t_0, T_{\max}]$ with the given discretization step $h = 1$ (day). So, we can assume the independent variable t and parameters τ , T , T_{\max} to be integer. The discrete function $K(i)$ is given for $i = 0, 1, \dots, T - \tau$.

Typical numerical discretization of the VIE-I leads to the system of linear algebraic equations with a lower-triangular matrix with small diagonal elements, that remains ill-posed. Consequently, our first attempts to solve the original VIE-I (3.3) using various numeric integration rules produced solutions β alternating between large negative and positive values because of fluctuations in the given I . In accordance with the epidemic meaning of the model, we restricted the calculated values $\beta(t)$ to an interval $[B_{\min}, B_{\max}] : 0 < B_{\min} \leq \beta(t) \leq B_{\max}$, but it was of a little help. Preliminary smoothing of the given function $I(t)$ was not enough either. The discretization of the regularized VIE-II (3.4) appears to be more successful and is described below.

Assuming that t is an integer and approximating the regularized VIE-II (3.4) with the rectangular integration rule, we obtain the system of linear algebraic equations

$$\alpha x(t) + \sum_{j=t-\widehat{T}}^{t-1} K(t-j)x(j) = I(t+\tau), \quad t = t_0 - \tau + 1, \dots, T_{max} - \tau. \quad (3.6)$$

From (3.6), we obtain the explicit formula for calculating the unknown $x(t)$:

$$x(t) = \frac{1}{\alpha} \left(I(t+\tau) - \sum_{j=t-\widehat{T}}^{t-1} K(t-j)x(j) \right) \quad (3.7)$$

for $t = t_0 - \tau + \widehat{T} + 1, \dots, t_{max} - \tau$. In the recurrent formula (3.7), $x(t)$ depends on \widehat{T} previous values $x(j)$, $j = t - 1, \dots, t - \widehat{T}$. To start calculations with (3.7), we use linear interpolation to determine the initial function

$$x(j) = x_0(j), \quad j = t_0 - \tau, \dots, t_0 - \tau + \widehat{T},$$

that satisfies the Equation (3.6) at $j = t_0 - \tau$.

For each t , we calculate $\beta(t) = I(t)S(t)x(t)/N$ and use the discretized equations (2.2) and (2.3) to find $R(t)$ and $S(t)$.

Without regularization parameter $\alpha > 0$, the discretized formula (3.7) is undefined because of the chosen discretization scheme for (3.4). Finding efficient values of the regularization parameter is the key challenge in solving ill-posed problems [6, 23]. Usually, accuracy of the data is not known, which makes theoretic approaches (convergency theorems) not applicable. An effective practical criterion for choosing regularization parameters is a visual control of the obtained solution when it is possible. Employing this idea, we can find the regularization parameter α^* that delivers the best correspondence between $I(t)$ recalculated below in Stage 2, and the original dataset vector for I .

Stage 2. Verification of solution and choice of regularization parameter.

This step verifies how accurately the solution β , obtained at a specific value α , satisfies the original model (2.1)–(2.3). Namely, we substitute the function $\beta(t)$, $t = t_0 - \tau, \dots, T_{max} - \tau$, obtained in Stage 1 to the discretized equations (2.1)–(2.3) and calculate the discrete functions $\widetilde{S}(t)$, $\widetilde{R}(t)$, and $\widetilde{I}(t)$ for $t = t_0 + T + 1, \dots, T_{max}$. In doing so, we use the known values of $S(t)$, $I(t)$, and $R(t)$ at $t = t_0, \dots, t_0 + T$ from Stage 1 as given initial conditions (2.4) on the prehistory of the process.

Next, we visually compare the calculated \widetilde{S} , \widetilde{I} , and \widetilde{R} with the given S , I , and R from the original dataset over the period $[t_0 + T, \dots, T_{max}]$. Starting with a small value $\alpha = 0.1$, we gradually increase it and repeat Stage 2, until we reach the best visual correspondence between the calculated $I(t)$, $t = t_0 + T, \dots, T_{max}$, and the original dataset curve I .

Calculations at Stage 2 can be unstable at the offset of epidemic when the given initial $I(t)$ is much smaller. We originally chose $t_0 =$ March 1, 2020, and $T_{max} =$ May 1, 2021 for the UK data. In the UK case, the number $I(t)$ of new

infected increases 40 times from 2.5 to 95 (per 1M) during 20 days from March 4 to March 20, 2020. As a result, we cannot reach an acceptable match (at any value α) if $t_0 =$ March 20. Then, Stage 2 is repeated with a new later date t_0 .

Solving the verification problem with the delayed $t_0 =$ May 1, 2020, demonstrates a much better agreement of $I(t)$ with original data over the period May 1, 2020–May 1, 2021, shown in Figure 3, with the average difference of 3-5% between the original and calculated values of I .

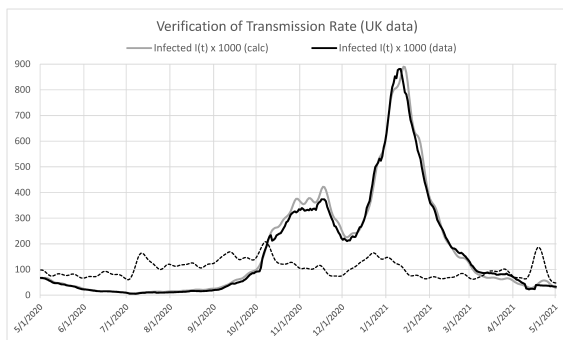


Figure 3. The observed and simulated dynamics of the new infected number in COVID-19 epidemic in the UK. The reproduction number (dotted curve) is found from the identification problem (3.1).

The best solution $\beta(t)$ of the identification problem on UK data is reached at $\alpha^* = 1.36$ and shown with solid black line in Figure 4. The corresponding reproduction number R_t is calculated using (2.7) and shown in Figure 4 with a dashed line.

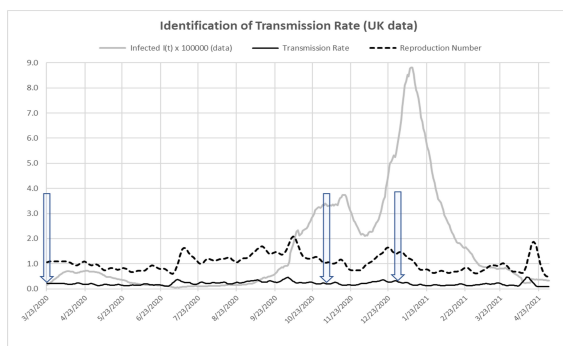


Figure 4. The identified transmission rate $\beta(t)$ and reproduction number R_t for COVID-19 epidemic in the UK in 2020-21. Three major lockdowns are indicated by arrows.

In summary, varying the value of regularization parameter α in (3.6), we have obtained an acceptable solution for the varying transmission coefficient $\beta(t)$ over the period of one year with several waves of COVID-19 in the UK.

4 Mitigation of COVID-19 epidemic in the UK: simulation and analysis

This section indicates how preventive actions instituted by the federal and local governments have affected the dynamics of the COVID-19 pandemic in the United Kingdom and its reproduction number R_t . The related information is obtained from online BBS News [7] and similar public sources.

The first wave and lockdown: March 2020–May 2020

The United Kingdom saw its first confirmed cases of COVID-19 in January 2020. In two weeks of March 8–22, the number of total cases in the UK increased 21 times from 7 to 153 cases (per million). On March 23, Prime Minister Boris Johnson issued the first stay-at-home order across the United Kingdom that closed non-essential businesses like restaurants and pubs, schools, churches, and prohibited gatherings of more than two unrelated individuals.

After the first lockdown, the number $I(t)$ of daily new cases continued to increase. In April 2020, the Prime Minister reported that the UK's lockdown measures had effectively “flattened the peak” of its COVID-19 outbreak, as $I(t)$ stabilized around 4500–5000 cases (per million) between April 6 and April 20, 2020. The maximum number of new cases on a single day during the first wave was 5505 per million on April 22. The UK saw $I(t)$ increased 100 times in less than two months during March 8–April 22.

The number of new cases began to decline in late April, but COVID-19 restrictions largely remained in place through May. A new COVID-19 alert system was announced to offer guidance based on the threat of the pandemic within individual sub-populations. The number $I(t)$ of new cases steadily decreased each week from April 22 to May 31 and was 1070 per million on May 31. Lockdown measures and testing were effective, so UK officials began planning for the country's reopening.

Lockdown lifting, slow reopening: June 2020–August 2020

As the number of COVID-19 cases continued to decline, the UK began to lift some of its COVID-19 restrictions. In June, children were able to return to school with continued social-distancing, churches and retail stores were able to open with capacity limits, and public recreational areas were reopened. The reproduction number was $R_t < 1$ from mid-May to July 6. The seven-day average $I(t)$ decreased from 22.7 in May 24–31 to 5.2 daily new cases (per million) in June 30–July 7. Local governments were responsible for enforcing mask mandates, social distancing measures, and capacity limitations.

Government preventative measures in the UK effectively reduced $I(t)$ in May and June, so the federal government began advocating for further reopening of the country. On July 4, the government reopened restaurants, pubs, cinemas, theme parks, beauty salons, and tattoo shops for the first time since March 2020. Although easing COVID-19 restrictions caused minor spikes in certain locations, the UK collectively saw a reduction in the number of new cases each day during June and July, with less than 1000 cases each day from June 19 to August 8 with only one exception, July 14. In late July, England mandates that masks must be worn in enclosed public spaces. Scotland began

requiring that masks be worn in shops.

In August, children returned to school without classroom capacity limitations. The federal government launched the “Eat Out to Help Out” campaign to encourage citizens to begin eating out again. July 7 was the first day that $R_t > 1$ in over two months. The reproduction number remained $R_t > 1$ for the most of July and August and the number of new cases per day began to increase faster in August.

The second wave and lockdown: September 2020–November 2020

The second wave of COVID-19 in the UK came as people began returning to their workplaces, children went back to school, and businesses began to reopen. The number $I(t)$ increased more than five times in two months: from 5 in June 30–July 7 to 27 new cases (per million people) in August 31–September 7.

The increase of $I(t)$ became more severe in September. In an attempt to curb the spike in the number of cases, the UK again limited social gatherings to six or fewer people. On September 22, Prime Minister ordered curfew for restaurants and pubs after 10 pm, a mask mandate in retail stores, and a 15-person limit on weddings. The number $I(t)$ continued to increase until November. Individual nations implemented further restrictions. Scotland instated a ban on visiting of multiple households indoors. On September 24, the NHS COVID-19 contact tracing app was released. Prime Minister Boris Johnson introduces a three-tiered system of restrictions.

From August to early November, R_t was larger than 1 across the UK. In early October, R_t was 1.3–1.6. On October 31, Prime Minister Boris Johnson declares the second lockdown for four weeks for England. It included mostly the same restrictions as the first lockdown in March: closing non-essential businesses, a stay-at-home order, and travel limitations. Schools remained open with after-school activities being suspended.

The number $I(t)$ reached the peak of its second wave the week of November 10–November 17, which averaged 373 daily new cases (per million). On November 27, $R_t < 1$ for the first time since August. Daily new cases decreased to 210 (per million) for the week of November 27–December 4. On December 2, the second lockdown was lifted and Pfizer/BioNTech vaccine rollout begins.

The third wave and lockdown: December 2020–March 2021

There was a little time between the second and third waves. On December 14, a new variant of COVID-19 was discovered in the UK and R_t rose above 1 again. On December 19, Prime Minister placed parts of England with high numbers of cases under strict lockdown once again. It included Scotland, Wales, Northern Ireland, and some cities in England. Still, many citizens traveled during Christmas break, leading to increased transmission. The number $I(t)$ continued to rise. R_t was estimated to be 1.9 on January 1, 2021.

To mitigate the COVID-19 spread, the UK instated the third national lockdown on January 4. This lockdown included a stay-at-home order, the closure of non-essential businesses and schools, and travel limitations. The UK saw the peak of its third wave in the week of January 3–January 10 with 881 average daily new cases (per million people).

The third lockdown was lifted gradually, in a similar way as was done for

the first lockdown. In late January, the UK has seen a reduction trend in the number $I(t)$ of new cases (except for some local areas). On January 22, $R_t < 1$ for the first time since early December and R_t continued to decrease in February as lockdowns persisted (and vaccines became available). On March 8, the UK opened schools once again, with regular testing for instructors and students. On March 29, the stay-at-home order was removed, and outdoor sports facilities reopened. Outdoor gatherings of at most six people or two households were permitted. Although COVID-19 restrictions were eased, $I(t)$ stayed low in March–April 2021.

Table 1 summarizes the timeline of UK government measures to mitigate three waves of COVID-19 epidemic over March 2020–March 2021. Times of three major lockdowns are indicated in Figure 4 by arrows. The table reveals relations between those measures and the dynamics of new cases and the calculated reproduction number.

Table 1. Timeline of COVID-19 spread and mitigation activities in the UK

Dates	Government measures	New cases	Reproduction Number
3/23/2020–5/9/2020	First lockdown: Stay-at-home order, School closures, Non-essential businesses closed	increases	>1 , 3/23/20–5/3/20 <1 , 5/4/20–7/5/20
5/10/2020–7/6/2020	Lockdown easing: Stores, schools, and other public spaces reopened. Social distancing. Mask mandates on public transit and in stores. Travel bans	decreases	<1 , 5/4/20–7/5/20
7/7/2020–11/5/2020	Slow Reopening: Restaurants, pubs, beauty salons, theme parks, and schools reopened	increases	>1 , 7/6/20–11/18/20
11/5/2020–12/2/2020	Second lockdown (in England): Stay-at-home order, Non-essential businesses closed	decreases	>1 , 11/5/20–11/18/20 <1 , 11/18/20–12/3/20
12/3/2020–1/3/2021	Lockdown easing (except for few hotspot cities). Citizens travel on holidays	increases	>1 , 12/5/20–1/3/21
1/4/2021–3/29/2021	Third lockdown: Stay-at-home order, School closures, Non-essential businesses closed)	decreases	>1 , 12/5/20–1/14/21 <1 , 1/15/21–4/10/21

5 Discussion and conclusions

Quantitative modeling of COVID-19 spread in different countries and regions is critical for proper assessment and implementation of government and public health actions to control COVID-19 pandemic. We contribute to this topic by

computing and analyzing a detailed timeline of the COVID-19 transmission rate and reproduction number in the UK over 2020–21. Among many related papers and public sources, only few provide such detailed timeline on real data, usually, without theoretical justification. Our analysis is based on the integral epidemiologic model (2.1)–(2.3) offered in [16] to analyze COVID-19 dynamics in the US. The time-varying transmission rate is found from the Volterra integral equation (3.4) of the first kind. Solving this equation on available COVID-19 data is challenging and requires special approaches. The present paper extends [16] and justifies an effective regularization algorithm for the identification of time-varying transmission rate in the model (2.1)–(2.3). The algorithm preserves the Volterra structure of the Equation (3.3). Our approach is close to the well-known discrete statistical technique [12] that estimates the epidemic reproduction number using clinical infectivity distributions. However, our formulation of the epidemic model in continuous time allows a deeper analysis using calculus tools and effective numeric solution using well-developed regularization methods.

The developed algorithm is tested on COVID-19 epidemic data in the UK in 2020–21. The calculated transmission rate is verified by substitution it to back to the model. We obtain extremely close qualitative and quantitative resemblance between the original and calculated numbers of infected individuals (shown in Figure 3), which confirms the effectiveness of the offered technique. Simulated dynamics of the reproduction number well matches the public data about related UK government actions to mitigate the epidemic.

Future research directions include advancing both the model and methods of its analysis.

- First, there exist other promising regularization approaches [23] to further improve the developed identification algorithm.
- Second, the epidemic model (2.1)–(2.3) is limited by the assumption that a population is a homogenous mix of individuals. A prospective extension would be to implement the metapopulation approach to COVID-19 epidemics. Structured metapopulation models [26] account for the characteristics of specific sub-populations within the population. In particular, studies using such models [1] categorized individuals in different age groups and revealed new effects of certain preventative measures such as stay-at-home orders.
- Finally, extending the optimization analysis of epidemic control actions in SIR models [1, 2, 5, 13] to the integral model (2.1)–(2.3) may lead to new theoretic insight into the effectiveness of government controls in mitigating epidemics.

Acknowledgements

The authors would like to thank two anonymous reviewers for comments. This research was partially supported by REU Site: Mathematical Modeling in the Sciences (NSF grant DMS-1950677) and PVAMU FEP and sabbatical leave.

References

- [1] D. Acemoglu, V. Chernozhukov, I. Werning and M. Whinston. *Optimal targeted lockdowns in a multi-group SIR model. Working Paper 27102*. National Bureau of Economic Research, Cambridge, 2020. <https://doi.org/10.3386/w27102>.
- [2] F.E. Alvarez, D. Argente and F. Lippi. *A simple planning problem for COVID-19 lockdown. Working Paper 26981*. National Bureau of Economic Research, Cambridge, 2020. <https://doi.org/10.3386/w26981>.
- [3] S. Anita. *Analysis and Control of Age-Dependent Population Dynamics*. Kluwer Academic Publishers, Dordrecht, 2000.
- [4] J. Arino and S. Portet. A simple model for COVID-19. *Infectious Disease Modelling*, **5**:309–315, 2020. <https://doi.org/10.1016/j.idm.2020.04.002>.
- [5] A. Atkeson. *What will be the economic impact of COVID-19 in the US? Rough Estimates of Disease Scenarios. Working Paper 26867*. National Bureau of Economic Research, Cambridge, 2020. <https://doi.org/10.3386/w26867>.
- [6] C.T.H. Baker. Methods for Volterra equations of first kind. In C.T.H. Baker(Ed.), *Numerical Solution of Integral Equations*, pp. 162–174. Clarendon Press, Oxford, 1974.
- [7] B. Barlow. R number for UK below 1 for first time since August. *BBC News*, 2020. Available from Internet: <https://www.bbc.com/news/health-55105285>. Accessed 4 July 2021
- [8] A. Bergman, Y. Sella, P. Agre and A. Casadevall. Oscillations in U.S. COVID-19 incidence and mortality data reflect diagnostic and reporting factors. *mSystems*, **5**(4):e00544–20, 2020. <https://doi.org/10.1128/mSystems.00544-20>.
- [9] F. Brauer, S. Castillo-Chavez and Z. Feng. *Mathematical Models in Epidemiology*. Springer, New York, 2019. <https://doi.org/10.1007/978-1-4939-9828-9>.
- [10] D. Breda, O. Diekmann, W. de Graaf, A. Pugliese and R. Vermiglio. On the formulation of epidemic models (an appraisal of Kermack and McKendrick). *J. Biol. Dynamics*, **6**(2):103–117, 2012. <https://doi.org/10.1080/17513758.2012.716454>.
- [11] C. Corduneanu. *Integral Equations and Applications*. Cambridge University Press, Cambridge, 1991. <https://doi.org/10.1017/CBO9780511569395>.
- [12] A. Cori, N.M. Ferguson, C. Fraser and S. Cauchemez. A new framework and software to estimate time-varying reproduction numbers during epidemics. *Amer. J. Epidemiology*, **178**(9):1505–1512, 2013. <https://doi.org/10.1093/aje/kwt133>.
- [13] J. Fernandez-Villaverde and C.J. Jones. *Estimating and simulating a SIRD model of COVID-19 for many countries, states, and cities. Working Paper 27128*. National Bureau of Economic Research, Cambridge, 2020. <https://doi.org/10.3386/w27128>.
- [14] H.W. Hethcote. The mathematics of infectious diseases. *SIAM Review*, **42**(4):599–653, 2000. <https://doi.org/10.1137/S0036144500371907>.
- [15] N. Hritonenko, V. Hritonenko and Y. Yatsenko. A review of epidemiologic models: from SIR to distributed delays. *An. Stiint. Univ. Al. I. Cuza Iasi. Mat.*, **66**(2):237–249, 2020.
- [16] N. Hritonenko, O. Yatsenko and Y. Yatsenko. Model with transmission delays for COVID-19 control: Theory and empirical assessment. *J. Public Econ Theory*, 2021. <https://doi.org/10.1111/jpet.12554>.

- [17] N. Hritonenko and Y. Yatsenko. Optimization of harvesting age in integral age-dependent model of population dynamics. *Math Biosciences*, **195**:154–167, 2005. <https://doi.org/10.1016/j.mbs.2005.03.001>.
- [18] N. Hritonenko and Y. Yatsenko. Bifurcations in nonlinear integral models of biological systems. *Internat. J. Systems Science*, **38**:389–399, 2007. <https://doi.org/10.1080/00207720701245544>.
- [19] N. Hritonenko and Y. Yatsenko. *Mathematical Modeling in Economics, Ecology and the Environment, Second Ed.* Springer, Massachusetts, 2013. <https://doi.org/10.1007/978-1-4614-9311-2>.
- [20] N. Hritonenko and Y. Yatsenko. Nonlinear integral models with delays: recent developments and applications. *J. King Saud University - Science*, **32**(1):726–731, 2020. <https://doi.org/10.1016/j.jksus.2018.11.001>.
- [21] M. Iannelli and F. Milner. *The Basic Approach to Age-Structured Population Dynamics. Models, Methods and Numerics.* Springer, Massachusetts, 2017. <https://doi.org/10.1007/978-94-024-1146-1>.
- [22] W.O. Kermack and A.G. McKendrick. A contribution to the mathematical theory of epidemics. *Proc. Roy. Soc. Lond. A*, **115**:700–721, 1927. <https://doi.org/10.1098/rspa.1927.0118>.
- [23] P.K. Lamm. A survey of regularization methods for first-kind Volterra equations. In D. Colton et al(Ed.), *Surveys on Solution Methods for Inverse Problems*, pp. 53–82. Springer, Wien, New York, 2000. https://doi.org/10.1007/978-3-7091-6296-5_4.
- [24] P. Linz. The solution of Volterra equations of the first kind in the presence of large uncertainties. In P. Linz(Ed.), *Treatment of Integral Equations by Numerical Methods*, pp. 123–130. Academic Press, London, 1982.
- [25] A.L. Lloyd. Realistic distributions of infectious periods in epidemic models: Changing patterns of persistence and dynamics. *Theoretic Population Biology*, **60**:59–71, 2001. <https://doi.org/10.1006/tpbi.2001.1525>.
- [26] M. Martcheva. *An Introduction to Mathematical Epidemiology.* Springer, Massachusetts, 2015. <https://doi.org/10.1007/978-1-4899-7612-3>.
- [27] OurWorldinData.org. Daily confirmed COVID-19 deaths, rolling 3-day average. *Our World in Data*, 2021. Available from Internet: <https://ourworldindata.org/grapher/daily-covid-deaths-7-day?tab=chart>. Accessed 29 March 2022
- [28] V.O. Sergeev. Regularization of Volterra equations of the first kind. *Soviet Math. Dokl*, **12**:501–505, 1971.
- [29] J.J.A. van Kampen, D. van de Vijver and P.L.A. Fraaij. Duration and key determinants of infectious virus shedding in hospitalized patients with coronavirus disease-2019 (COVID-19). *Nature Communications*, **12**:267, 2021. <https://doi.org/10.1038/s41467-020-20568-4>.
- [30] V. Volterra. *Theory of Functionals and of Integral and Integro-differential Equations.* Blackie & Son Limited, London, 1930.